

Simulation and risk analysis of dam failure in small terrace reservoirs in hilly areas

Hu Liu¹, Guoqing Sang¹, Wei Liu²

¹School of Water Conservancy and Environment, University of Jinan, Jinan, China;²Hydrological Center of Shandong Province, Jinan, China

Abstract. This study uses numerical simulation to analyse the dam failure and risk of small series (parallel) reservoir clusters in the hilly areas of China. Four small series (parallel) reservoirs in the Guozhuang River basin of Tai'an City are used as the target of the study, and a two-dimensional hydrodynamic reservoir failure numerical model was constructed to analyse the riskiness of various series (parallel) dam failure scenarios. The results of the analysis can provide some technical support for the forecasting and scheduling of small terrace reservoirs in hilly areas.

1 Introduction

In recent years, climate anomalies and extreme weather events have been frequent. The spatial and temporal distribution of precipitation has been seriously uneven, with record rainfall in many places. As a water hub that undertakes multiple functions such as flood control, irrigation, water supply and ecology, reservoirs are important infrastructures to ensure regional economic and social development. The majority of them are managed by townships or village collectives, and are affected by historical conditions and insufficient investment.

Due to the suddenness of the event, there is little historical research on the measured data of dam failure floods, which are now usually studied using numerical calculations or physical model tests.

In 1871, the French mechanic Saint-Venant proposed a system of Saint-Venant equations[1]. In 1892, the German scholar Ritter obtained a simplified solution for free outflow in rectangular river valleys[2]. In 1949, Schoklitch obtained an empirical formula for the calculation of the peak flow at a dam site in the event of an instantaneous partial breach[3]. In 1951, Frank derived the equation based on the Ritter instantaneous total breach solution[4]. In 1970, Su et al. applied the regressive solution to triangular, rectangular and parabolic cross-section open channels[5]. In 1980, Chen[6] In 1982 and 1984, Hunt et al. considered the effect of friction on the dam-break problem for finite-length reservoirs[7]. In 1986, Wu Chao and Tan Zhenhong[8] In 1986, Wu Chao and Tan Zhenhong derived a simplified solution for the U-shaped section dam-break wave by using the Riemann equation. 1999, WuC[9] In 2001, Yan Echuan et al. derived an equation for the peak flow of a lateral partial breach of a flat-bottomed unresisted river dam[10]. Although some research results have also been published on dam failure in groups of terraced reservoirs[11-16],

they mainly focus on the discussion of the dam failure flow equation, while the numerical simulation of dam failure floods and the analysis of the inundation risk to the downstream areas need to be further explored and studied.

Therefore, this paper takes four small reservoirs in series (parallel) in the Gozhuang River sub-basin of Geshishi Town, Ningyang County, Tai'an City, Shandong Province as the research object, and constructs a two-dimensional hydrodynamic model to numerically simulate different reservoir combinations with various dam failure scenarios. The results of the study can provide a reference basis for the safe scheduling and operation of reservoirs in the basin, the planning of downstream areas, flood warning and the formulation of dam failure countermeasures, and are of great theoretical and practical significance.

2 Overview of the study area

The Guozhuang River basin is located in Ningyang County, Tai'an City, Shandong Province across Ge Shi Town and Mound Town, with a basin area of 23.54km². The upstream of the Guozhuang River is the Xing Shan Reservoir, which is divided into two branches at He Wa Village. The south branch of the Guozhuang River is 1.43km from the bifurcation and 2.66km from the Xing Shan Reservoir dam site; the south branch of the Guozhuang River is 1.58km upstream from the Xing Shan Southwest Reservoir dam site, 3.01km from the bifurcation and 4.24km from the Xing Shan Reservoir dam site. The north and south branches of the Guozhuang River converge at Maozhuang Qiaobei Village and join the Shiji River in the south of Da'an Village.

Table 1. Table of reservoir parameters in the study area.

Reservoir name	Size	Longitude	Latitude	Total storage capacity (million m ³)	Dam height (m)	Dam type
Hing Shan Reservoir	Small (1)	116.905687	35.838623	223.23	12.5	Earth and stone dam
Hing Shan South West Reservoir	Small (2)	116.899021	35.819648	18.2	4.55	Earth and stone dam
Xuying Reservoir	Small (2)	116.876725	35.822574	62.5	7.33	Earth and stone dam
Xuying Southeast Reservoir	Small (2)	116.884489	35.815214	23.4	4.83	Earth and stone dam

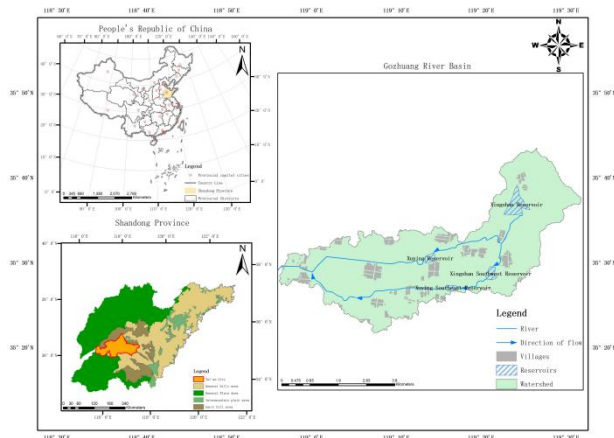


Fig. 1. Overview map of the study area.

3 Mathematical model construction

3.1. Model scope and main boundary conditions

The calculation area is based on the watershed boundary of the Guozhuang River, specifically from the east to the east of the village of Xingshanzhuang, from the west to the confluence of the Yueya River and the Shiji River, from the north to the south of the dam site of the Yueya River Reservoir and from the south to the Shiji River. The calculated area is 38.62km².

The two-dimensional hydrodynamic model uses an irregular grid. According to the requirements of the Technical Rules for the Preparation of Flood Risk Maps (for trial implementation), the maximum grid area should not exceed 0.1km² for irregular grids. Taking into account the model area, simulation accuracy, calculation time and software performance, for embankments, roads and other areas with drastic topographic changes, the calculation grid is appropriately encrypted under the premise of model stability; near the river channel, the buffer line of the Guozhuang River is buffered outward for 200m for encryption, and the maximum grid area within the buffer line is limited to 0.0001km², while the maximum grid area of the model area outside the buffer line is limited to 0.005km². The maximum grid area in the buffer line is limited to 0.0001km², and the maximum area of the model area outside the buffer line is limited to 0.005km². The mesh used for the calculation was generated by Mesh generator, with a total of 2357996 meshes and 118370 nodes. The elevation points used for terrain interpolation were extracted from the 5mDEM, and the river

embankments and main roads were corrected according to the supplementary survey data. A total of 619,000 elevation scatter points were extracted, with a spacing of 5m for rivers, embankments and roads and 10m for other features.

As all four reservoir dam types in the study area are earth and rock dams, this earth and rock dam breach was treated as an instantaneous lateral partial breach according to the Hydraulic Calculation Manual (2nd Edition).

(1) Dam breach width

Earthen dams are poorly resistant to scouring, and there is actual evidence that the breach will scour to the base of the dam or even form a local scour pit. The following calculation method is recommended by the Yellow Commission's Institute of Water Sciences based on the analysis of actual data.

$$b = k(V^{0.5}B^{0.5}H)^{0.5} \quad (1)$$

where: b - average width of the mouth door (m).

V - reservoir capacity at the time of dam breach (million m³).

H - depth of water in front of the dam at the time of breach (m).

k - coefficient related to the soil quality of the dam, with k values of approximately 0.65 for clayey soils and 1.3 for loamy soils.

B - the width of the water surface along the dam axis or the length of the top of the dam when the dam breaks m. If the width of the water surface in the reservoir area at the dam site section is greater than the length of the dam, the width of the water surface in the reservoir area at the dam site section should be used. If the water surface in the reservoir area is wider than the dam length, the width of the water surface in the reservoir area at the dam site section shall be used.

(2) Dam breach flow

The instantaneous lateral partial breach of a rectangular breach is chosen for the calculation of earth and rock dam failure floods. As the breach b is smaller than the dam length B, this negative wave upstream of the breach will have the characteristic of providing water discharge in multiple directions, thus increasing the depth of the breach and consequently the flow rate. The maximum flow cannot be calculated directly using the instantaneous total dam break, but needs to be multiplied by a correction factor greater than $1(\frac{B}{b})^\alpha$. The exponent of the correction factor, α , is generally taken to be 0.25-0.4. In this case, $\alpha = 0.4$ based on experimental data from the overall model of the Yellow Commission dam failure flood evolution.

$$b = k(V^{0.5} B^{0.5} H)^{0.5} Q_m = \frac{8}{27} \sqrt{g} \left(\frac{B}{b}\right)^{0.4} b H^{\frac{3}{2}} = 0.928 \left(\frac{B}{b}\right)^{0.4} b H^{\frac{3}{2}} \quad (2)$$

(3) Dam failure flood process

This time a quadratic parabola is used to generalise the flow process.

Table 2. Quadruple parabola table.

t/	0	0	0	0	0.	0.	0.	0.	0.	0.	1
T	0	1	2	3	4	5	6	7	8	9	5
Q	0	0	0	0	0.	0.	0.	0.	0.	0.	Q
/	2	1	1	0	0	0	0/
Q	1	6	4	3	2	0	6	3	9	6	3
m	2	8	4	6	7	8	0	4	1	0	M

1) Preliminary determination of the drainage time T from Qm and V.

$$T = K \frac{V}{Q_m} \quad (3)$$

Where: K - coefficient, generally take 4 to 5.

V - reservoir dischargeable volume before dam failure (m³)

2) Initially determine the flow process line from Table 3.3-1 based on T, Qm and Q0.

Check whether the water volume between the process line and the Q=Q0 line is equal to the dischargeable volume V. If it is not equal, adjust the T-value and retry the calculation until they are equal.

3.2 Working condition settings

In order to study different dam-break scenarios for small clusters of terraced reservoirs in hilly areas and their impact on disaster prevention objects in the downstream basin, this paper designs 10 series and parallel scenarios including single reservoir breaches and multiple reservoir breaches, as detailed in Table 3.

Table 3. Dam breach scenarios.

Condition No.	Dam failure forms
1	Dam Failure at Xing Shan Reservoir
2	Dam failure at Xuying Reservoir
3	Dam failure at Xing Shan South West Reservoir
4	Dam failure at Xu Ying southeast reservoir
5	Xing Shan reservoir dam failure flow leads to Xu Ying dam failure
6	Xing Shan Reservoir dam failure flow leads to dam failure at Apricot Hill Southwest Reservoir
7	Southwest Xing Shan reservoir dam failure flow leads to southeast Xu Ying reservoir dam failure
8	Simultaneous dam failure at Xing Shan Southwest Reservoir and Xu Ying Southeast Reservoir
9	The Xing Shan Reservoir dam failure flow leads to the Xing Shan Southwest Reservoir dam failure, which in turn leads to the Xu Ying Southeast Reservoir dam failure
10	The dam flow from the Xing Shan Southwest Reservoir leads to the failure of the Xu Ying and Xing Shan Southwest Reservoirs, which in turn leads to the failure of the Xu Ying Southeast Reservoir

4 Analysis of the simulation results of the dam failure flood

4.1 Analysis of the flow processes in the different scenarios of routing

The analysis of breach flow characteristics is the main research content of the breach flood, and the analysis of the maximum flow of the breach flood is an important work in the flood control planning and engineering design and construction of the downstream urban areas of the reservoir, and the breach flow can reflect the great destructiveness of the breach flood. Based on the 10 dam breach scenarios developed, the flood flow process at the breach was analysed and calculated for each scenario, and the flow process line at the breach is shown in Figure 2.

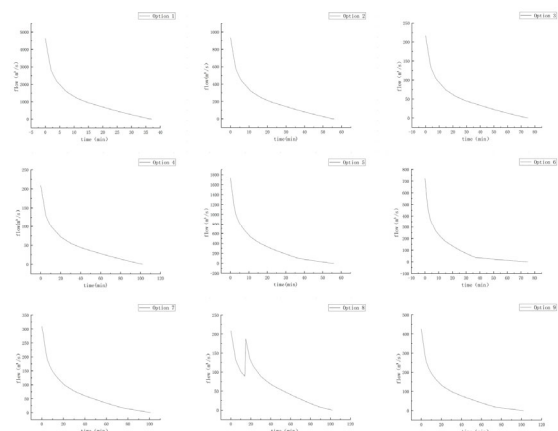


Fig. 2. Flow process lines at the breach for different scenarios.

The different scenarios show a single wave propagation downstream, with the maximum flow at the beginning of the breach when the breach occurs and then decreasing rapidly thereafter. The comparison of the different scenarios shows that the larger the reservoir capacity and the higher the dam site, the higher the breach flow. From scenarios 2 and 5, 3 and 6, 4 and 7 and 9, it can be seen that when there is a succession of breaches in the upstream gradient reservoirs, the resulting breached flow is greater than when there is a single reservoir breach, because as the breached flow evolves in the upstream reservoirs to the downstream reservoirs, the breached flow peaks will be superimposed and will be greater than the individual breached flows in the downstream reservoirs. As can be seen from Scenarios 4 and 8, the flow flood peaks from the simultaneous breach of the upstream and downstream reservoirs do not have a significant impact on the flow flood peaks from the separate breach of the downstream reservoirs. The distance between the two reservoirs is 1.58km. When the two reservoirs are breached at the same time, the peak flow will be significantly reduced during the evolution of the upstream reservoir breaching flood into the downstream reservoir due to the river roughness. The flood peak will then be smaller than its own peak flow.

Table 4. Table of parameters characterising the breach under different scenarios.

Progr amme	Water depth in front of dam (m)	Width of breach (m)	Maximum flood flow (m ³ /s)
1	12.5	42.19	4632.92
2	7.33	19.42	935.77
3	4.55	9.51	216.89
4	4.83	9.57	208.92
5	12.5/7.33	42.19/19.42	1735.93
6	12.5/4.55	42.19/9.51	721.97
7	12.5/4.83	42.19/9.57	309.67
8	4.55/4.83	9.51/9.57	208.92
9	12.5/4.55/4.83	42.19/9.51/9.57	425.80
10	12.5/7.33/4.55/4.83	42.19/19.42/9.51/9.57	1735.93/425.8

4.2. Analysis of the maximum flow along the route of the dam failure flood for different scenarios

The peak flow is gradually reduced from the breach site onwards. The following is the trend of the peak flow for each representative section of the breach flood along the route of each scenario.

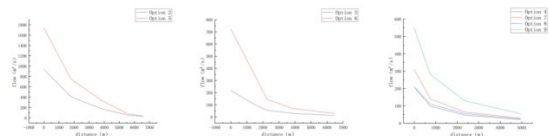


Fig. 3. Comparison of maximum flows along the length of the dam breach without options.

From options 2 and 5, 3 and 6, it is known that the upstream and downstream reservoirs collapse together compared to the downstream reservoirs collapse alone

The peak flows generated are not only the highest at the dam site, but also the maximum flows along the course of the flood as it evolves downstream. Moreover, the higher the peak flow generated by the successive breaches of the terrace reservoirs, the faster the receding rate during the evolution, but always greater than the single reservoir breach flow. As can be seen from Scenarios 4 and 8, the maximum flood flows are the same when the downstream reservoirs are breached alone and when the upstream and downstream gradient reservoirs are breached simultaneously, but the maximum alongstream flow is greater in the latter than in the former.

4.3 Analysis of inundated areas for different schemes

Table 5. Table of inundated areas under different working conditions.

Condition No.	1	2	3	4	5	6	7	8	9	10
Flooded area	15.29	4.46	1.57	1.7	5.17	3.25	2.39	2.37	2.94	18.25

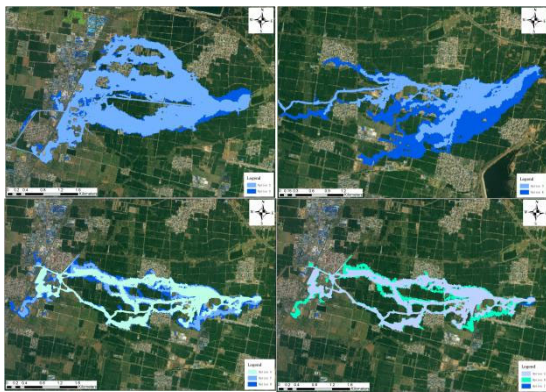


Fig. 4. Comparison of inundated areas for different scenarios.

Scenarios 2 and 5, 3 and 6, 4 and 7 and 9 show that the inundation area resulting from the successive breaches of the terrace reservoirs is greater than that resulting from the single breach of the downstream reservoirs. Comparing Scenario 4, Scenario 7 and Scenario 8, it is clear that the inundation area resulting from a downstream reservoir breach due to the flow of the upstream reservoir is greater than the inundation area resulting from a simultaneous breach of the upstream and downstream reservoirs, while the inundation area resulting from a simultaneous breach of the upstream and downstream reservoirs is greater than the inundation area resulting from a separate breach of the downstream reservoir. According to the analysis in

section 4.2, although the simultaneous dam failure in the upstream and downstream reservoirs produces a flood flow equal to the flood peak of the downstream reservoir alone, it is generated by the superposition of the two parts of the flood flow and therefore the flood volume is larger and the inundated area is greater.

4.4 Analysis of coastal village inundation impacts

The analysis of the two-dimensional dam failure flood calculation results shows that within the calculation range, the villages of Hehua, Xing Shanzhuang and Xiadaitang are closer to the Xing Shan reservoir dam site, and the leading edge and peak present time of the small reservoir dam failure flood is fast and the emergency response time is short, so it is necessary to develop a reasonable avoidance and relocation plan for the inundated villages. Given that scenario 10 caused the greatest inundation impact during this simulation, this most unfavourable scenario was considered for selection.

Of the inundated features, 90.9% were arable land and only 9.1% were residential land. In this simulation, 10 villages were inundated: Hewa, Xingshanzhuang, Xiadaitang, Wangjiashidai, Xujiaying, Shijie, Guozhuang, Xiningjiazhuang, Sujiazhuang and Maozhuangqiao North. Residents of He Wa and Heng Shan Zhuang can move southeast along the path up the mountain to settlement 1

near Dongliang Highway, while Xu Jiaying, Shijie Tun, Xia Dai Tang and Wang Jia Xia Dai can move along the path to settlement 2 on the high ground near Dongliang Highway between them, and Go Zhuang, Xining Jia Zhuang, Su Jia Zhuang and Mao Zhuang Qiao Bei villages can move to settlement 3 on the high ground near G342 in the west. The village of Hehua has the shortest emergency transfer time before the front edge of the flooding arrives, and should therefore respond quickly and move as soon as instructions to do so are received.

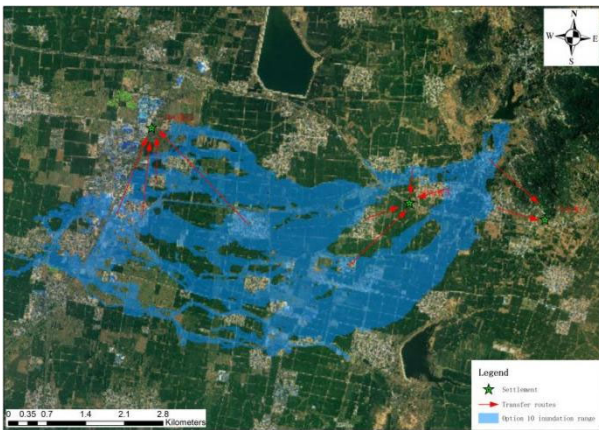


Fig. 5. Flood transfer route map.

5 Conclusion

In the analysis of the impact on downstream inundation in both single and continuous failure modes, all the conditions in this study show that when a single failure occurs in the downstream reservoirs, the maximum flow at the breach is greater than when a continuous failure occurs in the upstream and downstream terrace reservoirs, and the maximum flow along the course of the flood is also greater, and the impact on downstream inundation is more extensive in terms of area.

The conclusions drawn from this simulation comparing flood simulations in Scenario 7 and Scenario 8 are not generalisable. When the upstream and downstream gradient reservoirs are breached simultaneously, the final inundation results differ depending on multiple factors such as the maximum breach flow of the upstream and downstream reservoirs, the distance of the river between the two reservoirs and the impediment of the in-channel roughness to the rate of flood evolution, and should therefore be analysed on a case-by-case basis. If the upstream reservoir is large and the two reservoirs are close together, the impact on the downstream will be even greater if a succession of reservoir breaches occurs. Therefore, the study of graded reservoir breaches is of great significance for flood control and the protection of people's lives and property, and will be of great value for the development of flood evolution theory and engineering applications in the future.

Due to the complexity of the reservoir failure mechanism, different calculation methods yield different results. The calculation method used in this paper is relatively rough, and the results of the inundation analysis may be different from the actual situation, but it can

provide some reference for subsequent studies on the analysis of dam failure floods in terrace reservoirs.

Acknowledgments

The authors wish to gratefully acknowledge the financial assistance from the Natural Science Foundation of Shandong Province (ZR2020ME249) and the other anonymous reviewer whose comments greatly improved the quality of this paper.

References

1. Lh.Wang, Sy.Hu. Progress in Water Resources and Hydropower Science and Technology, A review of dam failure problems[J].(01): 80-5,(2007).
2. Zh.Chen,Kiselev.Hydropower,Handbook of hydraulic calculations [J]. (10): 44, (1957).
3. W.Cao. Taiyuan University of Technology, Numerical simulation and risk analysis of reservoir dam failure [D]. (2015).
4. Cj. Lee. Inner Mongolia Water Resources, Hydraulics of dam failure [J]. (04): 4, (1994).
5. Cl. Zhang, Cy. Zhu. Journal of Water Resources, (04): 80-4+62, (1997).
6. CHEN C L, ARMBRUSTER J F. Journal of Hydraulic Division, ARMBRUSTER J F. Dam-Break Wave Model: Formulation and Verification [J]. 106(5): 747-67, (1980).
7. HUNT B. Journal of Hydraulic Engineering, Dam-Break Solution [J]. (1984).
8. C. Wu, Zl. Tan. Journal of Chongqing Transportation Institute, Simplified calculation of U-shaped channel breach waves[J]. (03): 166-71, (1986).
9. WU C, HUANG G, ZHENG Y. Journal of Hydraulic Engineering, Theoretical Solution of Dam-Break Shock Wave [J]. 125(11), (1999).
10. Ec. Yan, Wm. Zheng, Hm. Tang., et al. Hydrogeology and engineering geology, Theoretical analysis of landslide dam failure floods and their evolution [J]. (06): 15-7+22,(2001).
11. Rh. Li. Hohai University, Generalized shallow water equations and preliminary research on engineering applications [D]. (2003).
12. Gq. Wang, Xd. Fu. Science Bulletin, The mechanism of vertical diffusion of sand-bearing water particles[J]. (04): 321-4,(2004).
13. Md. Zhao, Ll. Li., Xl. Zhou. China Rural Water Conservancy and Hydropower, Problems and corrections of the formula for calculating the maximum flow rate of a dam failure[J]. (06): 66-8, (2010).
14. Cy. Chen, Yq. Li, et al. Guangdong Water Conservancy and Hydropower, Calculation of continuous dam failure in a terrace reservoir [J]. (9): 40-42, 46, (2011).

15. B.Su. Henan Water Conservancy and South-North Water Diversion, Study on the calculation and impact scope of dam failure in a terrace reservoir [J]. (24) : 22-23, (2013).
16. L. Liu, Fx. Chang, Cw. Xiao, et al. Journal of the Changjiang Academy of Sciences, Progress in the study of dam failure flood [J]. 33 (6) : 29-35, (2016).